J Gynecol Oncol. 2021 May;32(3):e32
https://doi.org/10.3802/jgo.2021.32.e32
pISSN 2005-0380·eISSN 2005-0399

JOURNAL OF GYNECOLOGIC ONCOLOGY

Original Article

The prognostic significance of tumor-infiltrating lymphocytes in cervical cancer

Mengdi He [1,2,*] **Yiying Wang** [1,3,*] **Guodong Zhang** [1] **Kankan Cao** [1,3] **Moran Yang** [1,3] **Haiou Liu** [1,3]

[1]Obstetrics and Gynecology Hospital, Fudan University, Shanghai, China
[2]Department of Biochemistry and Molecular Biology, School of Basic Medical Sciences, Fudan University, Shanghai, China
[3]Shanghai Key Laboratory of Female Reproductive Endocrine Related Diseases, Obstetrics and Gynecology Hospital, Fudan University, Shanghai, China

Received: Jul 19, 2020
Revised: Dec 17, 2020
Accepted: Jan 2, 2021

Correspondence to
Haiou Liu
Shanghai Key Laboratory of Female Reproductive Endocrine Related Diseases, Obstetrics and Gynecology Hospital, Fudan University, Shanghai 200011, China.
E-mail: liuhaiou@fudan.edu.cn

*Mengdi He and Yiying Wang contributed equally to this work.

ORCID iDs
Mengdi He
https://orcid.org/0000-0003-2693-5261
Yiying Wang
https://orcid.org/0000-0002-9661-6111
Guodong Zhang
https://orcid.org/0000-0002-9297-1335
Kankan Cao
https://orcid.org/0000-0001-9242-1440
Moran Yang
https://orcid.org/0000-0002-0601-9090
Haiou Liu
https://orcid.org/0000-0003-0200-8981

ABSTRACT

Objective: To predict the prognosis of cervical cancer, we constructed a novel model with 5 specific cell types and identified a potential biomarker.
Methods: We employed CIBERSORT and xCell method to evaluate the abundances of 23 cells types in tumor microenvironment. Five specific cell types were filtrated to determine different immunotypes by applying least absolute shrinkage and selection operator (LASSO) Cox regression method. The expression of immune checkpoints (ICPs) and effectors were validated by immunohistochemistry. Correlation analysis was performed to examine the relevance between PIK3CA mutational status and ICPs.
Results: Unsupervised clustering of patients on the basis of tumor infiltrating lymphocytes and fibroblasts identified patients with shorter overall survival (OS) (hazard ratio [HR]=3.0729; 95% confidence interval [CI]=1.5103–6.2522; p=0.0118). An immunoscore (IS) signature consisting of 5 immune cell types infiltrating in tumor core (CD8T, activated NK cells, neutrophils, activated mast cells, macrophages) was constructed using LASSO Cox regression analysis. Receiver operating characteristic curves confirmed that the area under the curve of IS was significantly higher to that of International Federation of Gynecology and Obstetrics staging alone (0.637 vs. 0.55). Survival analysis revealed patients in high IS group exhibited a poorer OS (HR=3.0113; 95% CI=1.8746–4.8373; p<0.0001). The multivariate analysis indicated the IS was an independent prognostic factor. In addition, the lower IS related to higher expression of ICPs and neoantigen load.
Conclusions: The identification of IS in cervical cancer tissues could facilitate patient risk stratification and selection of immunotherapeutic responses, but more prospective studies are needed to assess its reliability.

Keywords: Cervical Cancer; Survival Analysis; Immune Checkpoints Molecules

INTRODUCTION

Cervical cancer is one of the common women malignant tumors around the world. It ranked fourth for incidence and was also the fourth leading cause of death among women [1]. Since human papillomavirus (HPV) vaccine has been explored and introduced in several countries,

Funding
This study was funded by grants from National Natural Science Foundation of China (82072881, 31570803 81773090), Natural Science Foundation of Shanghai (20ZR1409000), FDUROP (Fudan's Undergraduate Research Opportunities Program) (19055), and National University Student Innovation Program (19055).

Conflict of Interest
No potential conflict of interest relevant to this article was reported.

Author Contributions
Conceptualization: Z.G., L.H.; Data curation: H.M., W.Y., Z.G., L.H.; Formal analysis: W.Y.; Methodology: H.M., W.Y., Z.G., C.K., Y.M.; Project administration: L.H.; Supervision: L.H.; Validation: H.M., W.Y., Z.G., C.K., Y.M.; Visualization: H.M., W.Y.; Writing - original draft: H.M.; Writing - review & editing: L.H.

the incidence of cervical cancer has been decreasing in recent years [2]. In addition, there is still an unmet demand for treatments for patients of cervical cancer [3]. Therefore, new therapeutic strategies and novel biomarkers (including the ideal biomarkers for immunotherapy) that contribute to provide prognostic information are desperately needed, especially for advanced carcinoma of cervix.

Previous studies have demonstrated that heterogeneity of tumor microenvironment (TME) including immune infiltrating cells in cervical cancer may influence its development, occurrence, and prognosis [4,5]. However, the landscape of tumor infiltrating cells (TICs) associated with the prognosis of cervical cancer remains poorly described. A comprehensive grasp of TICs is conductive to predicting the disease prognosis and personalizing the treatments for patients of cervical cancer, for the reason that both immuno-suppressive and immuno-active cells were known for coordinating tumor progression and tumor metastasis [6]. On the other hand, despite there were several prognostic models of cervical cancer having been constructed, few combined multiple biomarkers into one single model [7-9]. Several studies have also observed that the method utilizing tumor infiltrating cells and fibrocytes (fibro) may constructed a better prognostic model in other cancers [10,11].

Therefore, in this study, we confirmed that 5 specific immune infiltrating cells participated in building a new prognostic model and a new immunoscore (IS) was identified as an independent prognostic factor. Patients in the low IS group exhibited a better overall survival (OS), and thus we performed immunohistochemistry (IHC) to define its characteristics. Additionally, a correlation among immuno-activity and immune checkpoints (ICPs) was discovered and validated. *PIK3CA*, as a potential biomarker, may conduce to predict survival and suggested its possibility of targeted therapy in cervical cancers [12-14].

MATERIALS AND METHODS

1. Cervical cancer datasets

In total, we gathered 3 cohorts of samples from patients for this study.

Cohort 1 raw data from The Cancer Genome Atlas (TCGA) were downloaded from the UCSC Xena browser (https://xenabrowser.net/datapages/). The selection criteria were: 1. Available for mRNA expression data. 2. Available for OS data. 3. Pathological type: cervical cancer. In addition, somatic mutation genes (SMGs) and neoantigen data in cervical cancer were respectively obtained from cBioPortal (http://www.cbioportal.org/) and The Cancer Immunome Atlas (https://tcia.at/).

Patients of Cohort 2 underwent cervical conization in Obstetrics and Gynecology Hospital, Fudan University were included. Pathology staging was performed according to the International Federation of Gynecology and Obstetrics (FIGO) classification (2018). Pathologic data consisted of histologic type and TNM staging were determined according to the current World Health Organization classification [15]. All the cases were reviewed and pathological diagnosis were confirmed by at least 2 gynecological pathologists. Cohort 2 was comprised of 63 cancers consisting of 6 HPV negative and 36 HPV positive (the rest were undetected), and 6 cervical intraepithelial neoplasms (CINs).

Cohort 3 raw data including GSE5787, GSE226511, GSE63514, GSE75132, GSE27678 from Affymetrix and Illumina microarrays were downloaded from the Gene Expression Omnibus (https://www.ncbi.nlm.nih.gov/geo/). The mRNA expression data from the same Affymetrix Human Genome U133 Plus 2.0 Array were altered to background-adjusted, quantile-normalized and log-transformed expression values using Robust Multichip Average expression summary in RMAExpress (version 1.2.0). The selection criteria were: 1. Available for mRNA expression data. 2. Pathological type: CIN or cervical cancer.

2. Gene expression data analysis

We first employed CIBERSORT method (https://cibersort.stanford.edu/) using the provided LM22 signature genes file (22 immune cell types) in Cohort 1 to evaluate the abundances of immune infiltrates in TME. Fibrocyte infiltrating data of Cohort 1 were obtained by applying xCell method (http://xcell.ucsf.edu/). Patients with different tumor infiltrating cell patterns including 22 immune cell types and fibrocyte [10] were grouped using Hierarchical Clustering (based on Euclidean Distance and Average linkage clustering). Least absolute shrinkage and selection operator (LASSO) Cox regression method [16] was used to remove redundant cells, as a consequence we selected 5 survival-related cells (neutrophils [Neut], mast activated cells [Masta], macrophages [M0], NK activated cells [NKa], CD8 T cells [CD8T]). The coefficients and partial likelihood deviance were calculated with "glmnet" package in R (version 3.6.1; R Foundation, Vienna, Austria). The formula was as follows: IS=1.011*Neut+5.393*Masta+0.542*M0+3.451*NKa–1.609*CD8T. Every sample was estimated by this formula and gained an IS. The cut off value was determined by the X-tile software (version 3.6.1; Yale University School of Medicine, New Haven, CT, USA). We chose the optimized value "0.48" by X-tile, as it could facilitate patient risk stratification (p=0.0003) and there was a nearly equals split between these 2 groups. For further analysis, MCP-counter method [17] was applied to evaluate the different immune infiltrates between these 2 groups.

3. Functional and pathway enrichment analysis

To determine the gene features of the 2 groups before (IS Lo, IS Hi), Gene Ontology (GO) terms were identified with a strict cutoff of $p<0.01$ and false discovery rate<0.05 [18]. We also identified pathways that were upregulated and downregulated between IS Lo and Hi Lo by running Gene Set Enrichment Analysis (GSEA) with differentially expressed genes (DEGs; DEGs between the groups were determined using the R package "limma"). Immune system process, on the basis of up-regulated genes in IS Lo, was performed by ClueGO (version 2.5.4).

4. IHC and evaluation

For IHC, tissue microarray (TMA) sections were performed through deparaffinizing, rehydrating, bringing slides to a boiled sodium citrate buffer then cooling down to room temperature, blocking each section with 100–200 μL blocking solution for 2 hour at room temperature, incubating primary antibodies with PD-1 (HPA035981, 1:100; Sigma, St. Louis, MO, USA), PD-L1 (SAB4301882, 1:60; Sigma), GZMB (46890s, 1:500; Cell Signaling Technology, Danvers, MA, USA), CD68 (ab955, 1:300; Abcam, Cambridge, UK), CD56 (07-5603, 1:600; Invitrogen, Carlsbad, CA, USA), CD8a (70306s, 1:200; Cell Signaling Technology), anti-Mast cell tryptase (ab2378, 1:10,000; Abcam), CD66b (392902, 1:400; Biolegend, San Diego, CA, USA) overnight at 4°C, adding secondary antibody and staining. All the slides were analyzed using National Institutes of Health software ImageJ (Java™ Platform SE binary; National Institutes of Health, Bethesda, MD, USA). We chose 3 high-power fields (HPF) of every point from TMA. Data of every point was hence evaluated and

recorded as the average number of positive cells per HPF. In particular, PD-L1 expression was evaluated respectively in tumor core region and stroma.

5. Statistical analysis

Statistical analysis was performed using R software (version 3.6.1; R Foundation) and Graphpad prism (version 8; GraphPad Software, San Diego, CA, USA). Cumulative survival was estimated applying the Kaplan-Meier method and the significance was assessed by the log-rank test. Chi-square test was used to examine the difference in clinical indicators between the 2 groups by IBM SPSS Statistics 21.0 (IBM Corp., Armonk, NY, USA). Both univariate and multivariate Cox proportional hazards regression analysis were applied to estimate the hazard ratios and 95% confidence intervals of IS and other clinical indicators (age, HPV status, clinical stage, histological type, TNM staging) by MedCalc (version 18; MedCalc Software, Mariakerke, Belgium). The receiver operating characteristic (ROC) curves and area under the curve (AUC) were performed and calculated by packages in R.

RESULTS

1. Specific immune infiltrating cells contributed to build new prognostic model

Cohort 1 was grouped in 3 clusters on the basis of different infiltrates of 23 cells: B naïve cells (Bn), B memory cells (Bm), plasma cells (plasma), CD8T, naïve CD4 T cells (CD4Tn), resting memory CD4 T cells (CD4Tm), activated memory CD4 T cells (CD4Tma), follicular helper T cells (Tfh), regulatory T cells (Tregs), γδT cells (Tgd), resting NK cells (NKr), activated NK cells (NKa), monocytes (mono), M0 macrophages (M0), M1 macrophages (M1), M2 macrophages (M2), resting dendritic cells (DCr), activated dendritic cells (DCa), resting mast cells (mastr), masta, eosinophils (eos), Neut and fibro. The clinical characteristics and pathological information for patients among 3 groups were displayed in **Fig. 1A** (**Supplementary Table 1**). Histological types were categorized as squamous cell carcinoma (SCC) and adenocarcinoma, of which 85.5%, 76.1%, 84.6% were observed for SCC in 3 groups (**Supplementary Fig. 1A**: p=0.199). Additionally, we analyzed HPV status, HPV types as well as their proportions in 3 clusters respectively (**Supplementary Fig. 1B**: p=0.273; **Supplementary Fig. 1C**: p=0.276). Patients of cluster 2 showed a better OS in Kaplan-Meier survival curve, compared with cluster 1 and 3 (**Fig. 1B**: p=0.0118).

Considering not all 23 cells were significantly associated with OS, we applied LASSO Cox regression method to filter related cells and their distribution. Five related immune infiltrating cells were selected from 23 tumor infiltrating cells to construct the prognostic model. The formula based on the coefficients and partial likelihood deviance from LASSO was as follows (**Fig 2A**): IS=1.011*Neut+5.393*Masta+0.542*M0+3.451*NKa−1.609*CD8T. According to the median IS (IS_{median}=0.048), Cohort 1 was split into 2 groups: IS Lo and IS Hi. The IS curve and patient survival status suggested that patients with lower IS tended to have a better prognosis (**Fig. 2B and C**), which corresponded with the result analyzed with 3 clusters: cluster 2 with the prolonged survival had the lowest IS (**Fig. 2E**) and a greater proportion of patients belonging to the low IS group (**Fig. 2F**). Moreover, CD8T were enriched in IS Lo, while macrophages and Neut were congregating in IS Lo (**Fig. 2D**). Distribution of clinical characteristics including FIGO staging (p=0.045) (**Fig. 2G**) and TNM staging (T: p=0.011; N: p=0.011, **Fig. 2H**; M: p=0.029) (**Supplementary Table 2**) varied significantly in IS Lo and IS Hi. In addition, MCP-counter method confirmed different immune infiltrating patterns

https://doi.org/10.3802/jgo.2021.32.e32

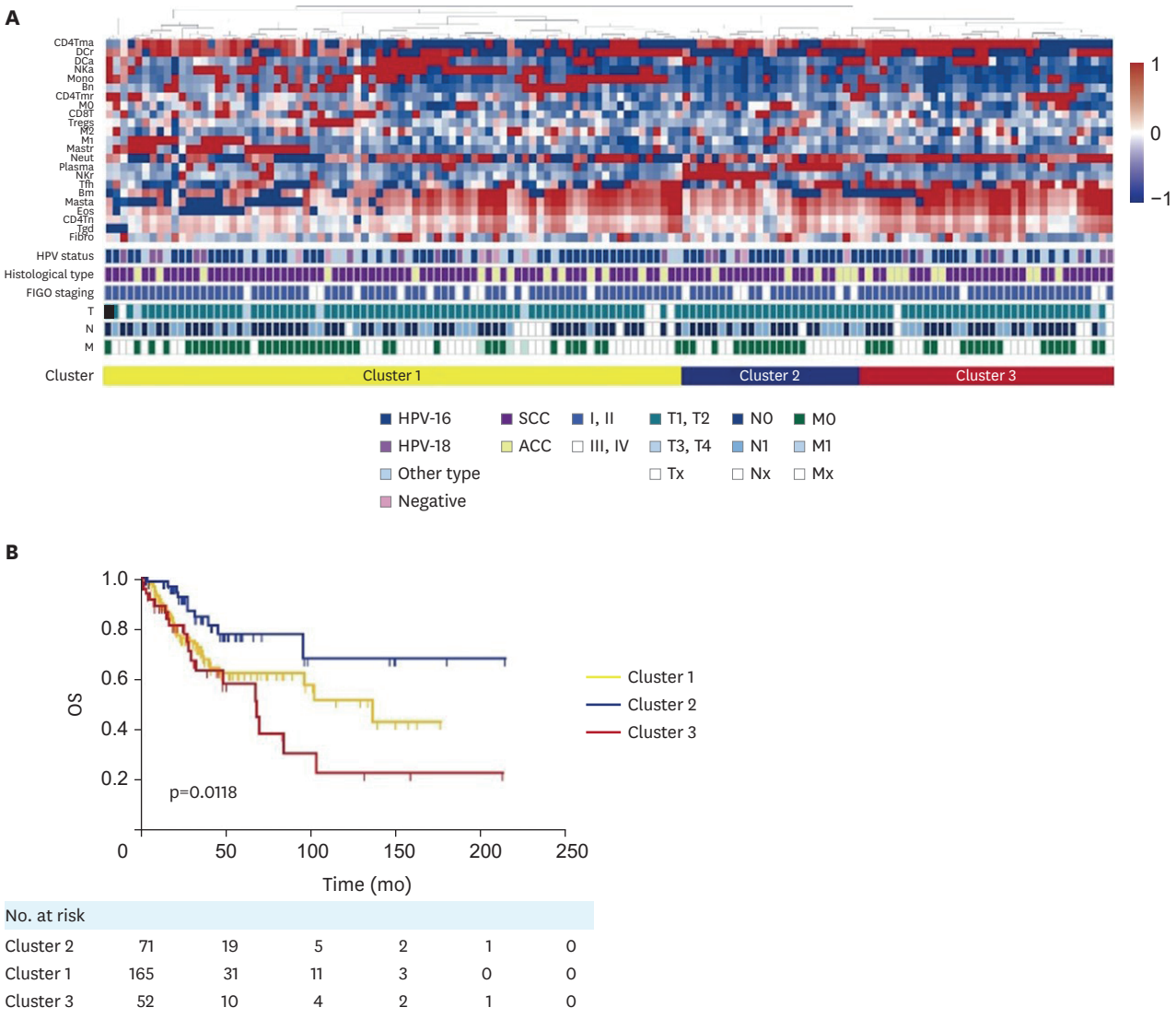

Fig. 1. Clinical information and survival analysis of 3 clusters based on immune infiltrates. (A) Tumor infiltrating cells, clinical and pathological features of 138 samples for 3 clusters in Cohort 1. (B) Kaplan-Meier survival curves displayed the clinical outcomes of 3 clusters.
ACC, adenocarcinoma; Bm, B memory cells; Bn, B naïve cells; CD4Tma, activated memory CD4 T cells; CD4Tmr, resting memory CD4 T cellls; CD4Tn, naïve CD4 T cells; CD8T, CD8 T cells; DCa, activated dendritic cells; DCr, resting dendritic cells; Eos, eosinophils; Fibro, fibrocytes; FIGO, International Federation of Gynecology and Obstetrics; HPV, human papillomavirus; M, metastasis; Masta, mast activated cells; Mastr, resting mast cells; Mono, monocytes; M0, M0 macrophages; M1, M1 macrophages; M2, M2 macrophages; N, node; Neut, neutrophils; NKa, NK activated cells; NKr, resting NK cells; Plasma, plasma cells; SCC, squamous cell carcinoma; T, tumor; Tfh, follicular helper T cells; Tgd, γδT cells; Treg, regulatory T cells.

in these 2 groups. On further analysis, all immune cells except myeloid DC, which were conventionally considered as essential roles in inhibiting tumor growth, were seen to be enriched in IS Lo (**Fig. 2I**). The reasons behind needed more study.

Compared with IS Hi, survival analysis suggested that low IS was a good prognostic indicator (**Fig. 3A**). Together with univariate, multivariate Cox regression analysis and risk stratification by FIGO staging (**Supplementary Fig. 1D-F**), we preliminary demonstrated that IS might be an independent prognostic index for OS in cervical cancer (**Fig. 3C**, **Supplementary Fig. 1D-F**). The AUC of the survival ROC reached 0.637 for IS, 0.55 for FIGO staging, indicating its satisfactory prognostic value of estimating patient survival (**Fig. 3B**).

https://doi.org/10.3802/jgo.2021.32.e32

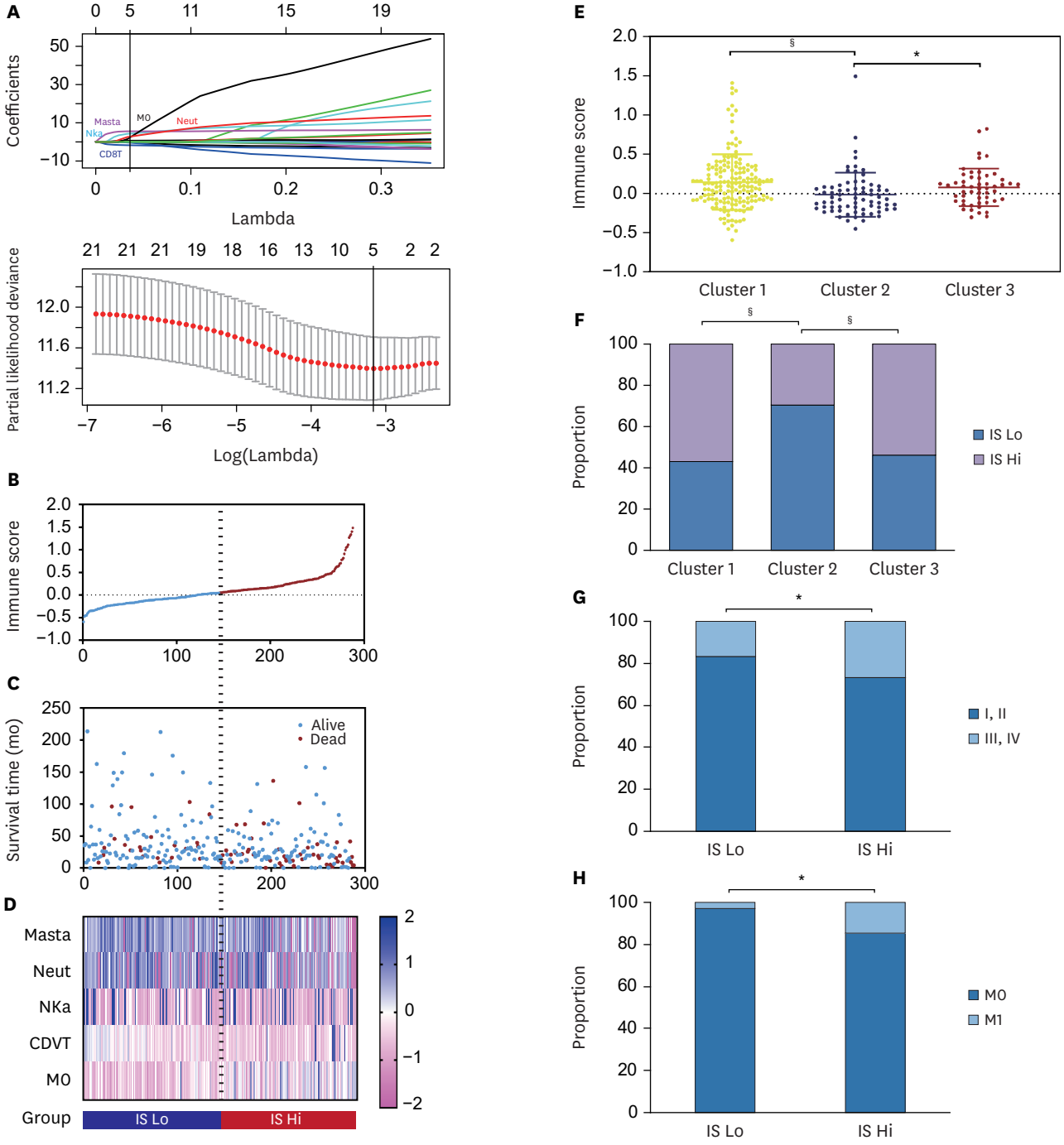

Fig. 2. Five specific immune infiltrating cells contribute to build the prognostic model. (A) Five immune infiltrating cells including Neut (red), Masta (purple), macrophages (black), NKa (light blue), CD8T (dark blue) were selected by LASSO Cox regression method. (B) IS, survival status and (C) OS time of patients in Cohort 1. (D) Heatmap of 5 immune infiltrating cells profiles (the transition from pink to blue suggested the transition from low proportion to high proportion). (E) Scatter plots showed cluster 2 had lower IS than cluster 1 and 3. (F) The histogram of immune type in 3 clusters. The histogram of (G) FIGO staging, (H) metastasis in IS Lo and IS Hi. (I) Violin plots of immune infiltrating cells between the 2 groups.
CD8T, CD8 T cells; FIGO, International Federation of Gynecology and Obstetrics; IS, immunoscore; LASSO, least absolute shrinkage and selection operator; Masta, mast activated cells; M0, M0 macrophages; Neut, neutrophils; NKa, NK activated cells; OS, overall survival.
ns, not significant; *p<0.05; ‡p<0.001; §p<0.0001.

(continued to the next page)

https://doi.org/10.3802/jgo.2021.32.e32

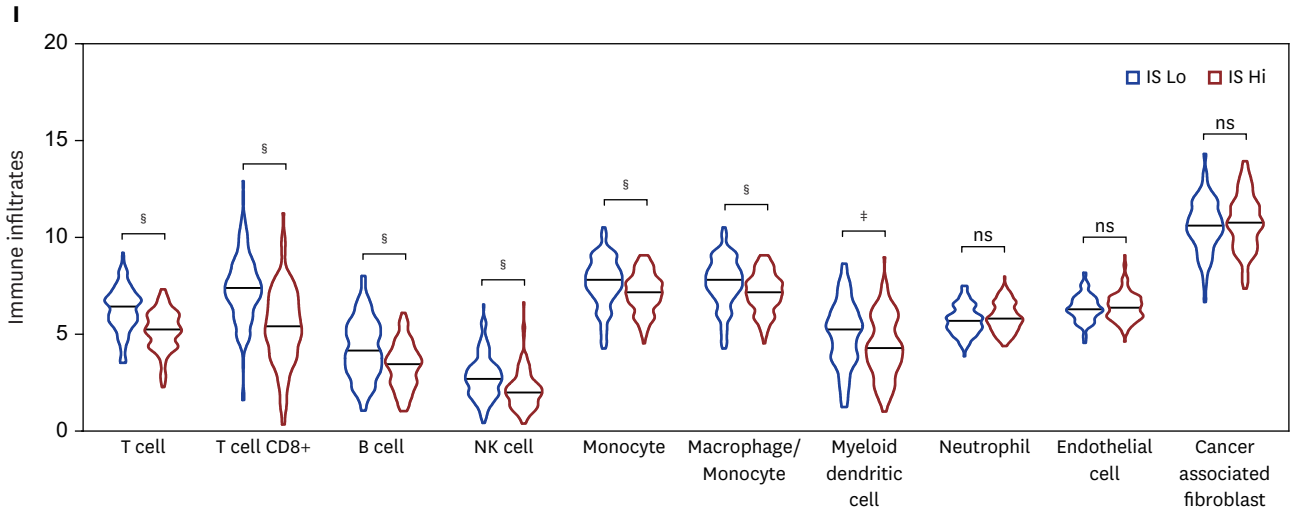

Fig. 2. (Continued) Five specific immune infiltrating cells contribute to build the prognostic model. (A) Five immune infiltrating cells including Neut (red), Masta (purple), macrophages (black), NKa (light blue), CD8T (dark blue) were selected by LASSO Cox regression method. (B) IS, survival status and (C) OS time of patients in Cohort 1. (D) Heatmap of 5 immune infiltrating cells profiles (the transition from pink to blue suggested the transition from low proportion to high proportion). (E) Scatter plots showed cluster 2 had lower IS than cluster 1 and 3. (F) The histogram of immune type in 3 clusters. The histogram of (G) FIGO staging, (H) metastasis in IS Lo and IS Hi. (I) Violin plots of immune infiltrating cells between the 2 groups.
CD8T, CD8 T cells; FIGO, International Federation of Gynecology and Obstetrics; IS, immunoscore; LASSO, least absolute shrinkage and selection operator; Masta, mast activated cells; M0, M0 macrophages; Neut, neutrophils; NKa, NK activated cells; OS, overall survival.
ns, not significant; *p<0.05; ‡p<0.001; §p<0.0001.

2. Analysis of the immunobiological characteristics and signal pathways of immunotypes

IS Lo exhibited distinct expression patterns for immune-specific gene sets. After comparing the mRNA expression levels of Cohort 1, 262 genes were identified as significantly differentially expressed between the 2 groups ($|\log_2 FC| \geq 1$, adj.p-value≤0.05). Meanwhile, the genes coding for ICPs (*PD-1*: $|\log_2 FC| = 1.731$) and effectors (*GZMB*: $|\log_2 FC| = 1.405$) were up-regulated in IS Lo (**Fig. 4A**). To determine pathways that were upregulated and downregulated in the 2 groups, we applied GSEA and GO analysis. The results displayed that IS Lo was highly enriched in the pathways including antigen processing and presentation, Toll-like receptor signaling, T-cell receptor signaling and B-cell receptor signaling, NK cell-mediated cytotoxicity, indicating its active immune status (**Fig. 4B**, **Supplementary Table 3**). Thus, tissues with lower IS had distinct immunobiological characteristics: higher expression of ICPs and up-regulation of immune-related pathways. Moreover, 7 classical ICPs and 2 immune effectors (CD8A, GZMB) expression profiles were compared in Cohort 1 between IS Lo and IS Hi (**Fig. 4C**). Notably, IS Lo maintained at a higher level of expression of ICPs and immune effectors, when compared to IS Hi (**Fig. 4D**).

Given that higher expression of ICPs was tightly related to immune activity, IHC was performed and we further analyzed the expression of every point on TMA (**Fig. 4E**). In cervical cancer, the results indicated that the expression of PD-1 was significantly and positively correlated with the expression of immune effector-GZMB (**Fig. 4F**). However, the expression of PD-L1 was far more complicated, for both cancer cells and tumor-infiltrating lymphocytes had variably PD-L1 positive expression. As a result, we evaluated every point in tumor core region and stroma, respectively (**Supplementary Fig. 2A-D**). In particular, the expression of PD-L1 were shown to be positively relevant to that of GZMB in total and stroma, while we didn't reach the similar conclusion in tumor core. Taken together, these results

https://doi.org/10.3802/jgo.2021.32.e32

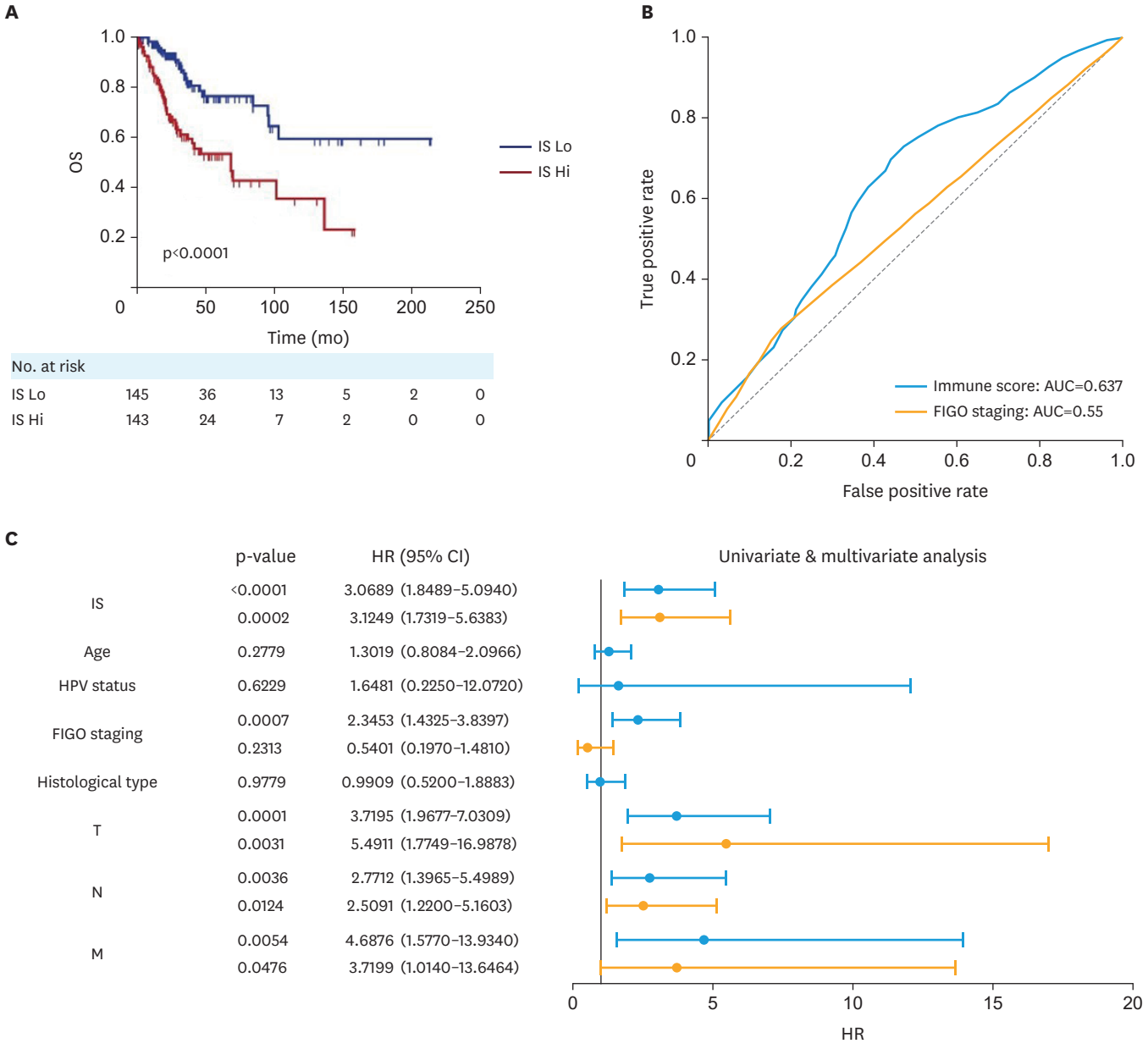

Fig. 3. Evaluation of the prognostic value of IS. (A) Kaplan-Meier survival curves displayed the clinical outcomes of the 2 groups. (B) ROC curves of survival prediction by indicators: IS (blue), FIGO staging (yellow). (C) Univariate and multivariate analysis of IS and other clinical indicators.
AUC, area under the curve; CI, confidence interval; FIGO, International Federation of Gynecology and Obstetrics; HPV, human papillomavirus; HR, hazard ratio; IS, immunoscore; M, metastasis; N, node; OS, overall survival; ROC, receiver operating characteristic; T, tumor.

suggested that higher expression of PD-1 and PD-L1 related to higher expression of GZMB, which might give partial interpretation to better prognosis of patients in IS Lo.

3. Different genomic characteristics in IS Lo vs. IS Hi

Additionally, we analyzed 272 samples. Several common somatic gene mutations, *PIK3CA*, was detected in 28% patients, followed by *EP300* (12%), *FBXW7* (11%), *PTEN* (7%), *ARID1A* (6%), *KRAS* (6%), respectively (**Fig. 5A**). Among 13 SMGs (*FBXW7*, *KRAS*, *MAPK1*, *PTEN*, *HLA-A*, *HLA-B*, *ARID1A*, *EP300*, *PIK3CA*, *NFE2L2*, *CASP8*, *ERBB3*, *STK11*) [19], except *MAPK1*, *PTEN*, *NFE2L2* and *STK11*, the majority were more frequently mutated in IS Lo. Considering

https://doi.org/10.3802/jgo.2021.32.e32

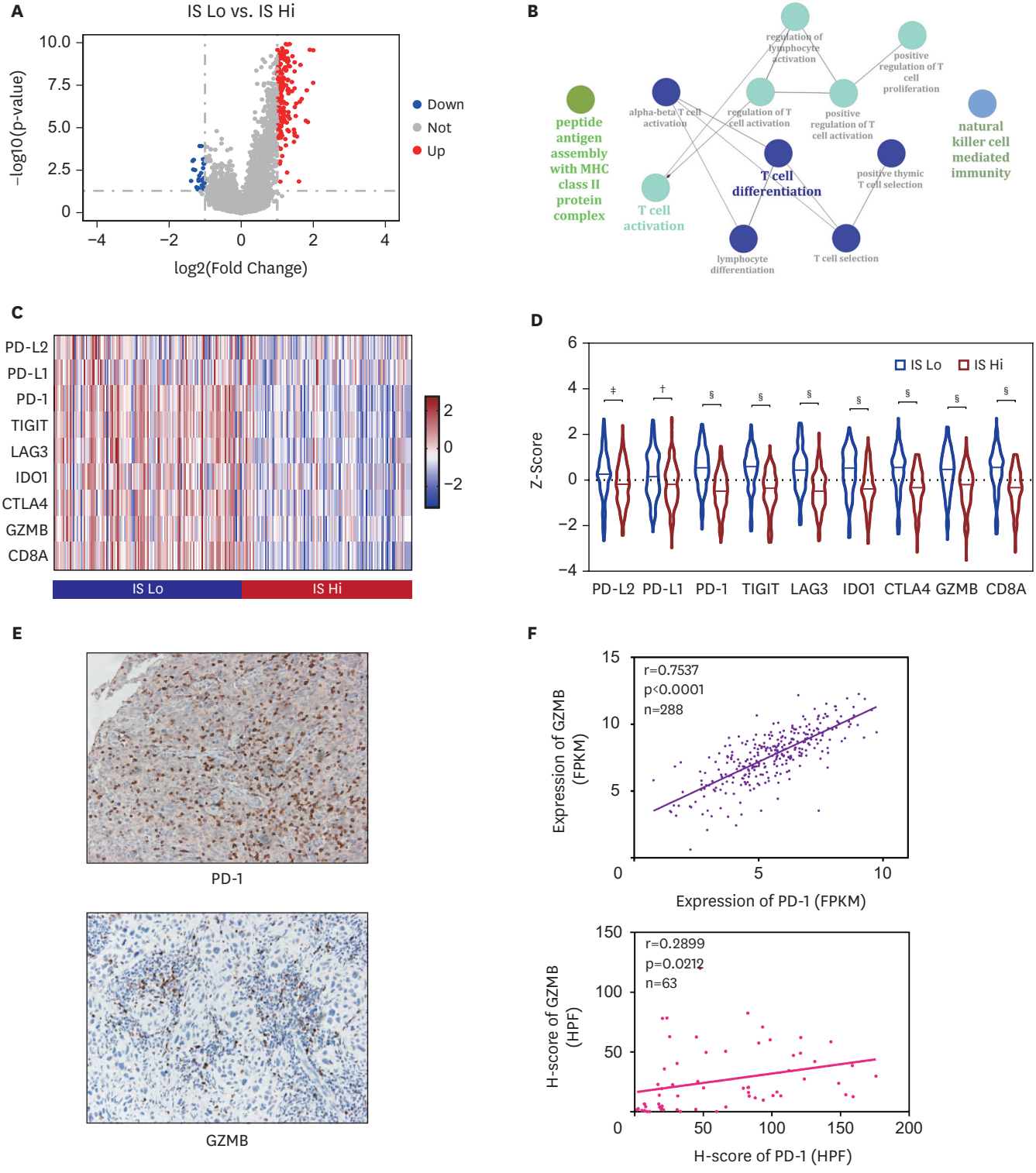

Fig. 4. Tissues with lower immune cell infiltrating score indicates a distinct immunobiology. (A) Volcano plot exhibited DEGs between IS Lo and IS Hi (red: up-regulated, blue: down-regulated, grey: no significance). (B) Network plot of immune system process that was up-regulated in IS Lo. (C) Heatmap of 7 ICPs and 2 effectors profiles. (D) Violin plots of ICPs and effectors between the 2 groups. (E) Images of IHC for PD-1, GZMB in TMA. (F) Correlations between PD-1 and GZMB in Cohort 1 and 2, respectively.
DEG, differentially expressed gene; HPF, high-power fields; ICP, immune checkpoint; IHC, immunohistochemistry; IS, immunoscore; TMA, tissue microarray.
*p<0.01; †p<0.001; ‡p<0.0001.

https://doi.org/10.3802/jgo.2021.32.e32

the polymorphism of *HLA* (*HLA-L*, *HLA-J*, *HLA-H*, *HLA-G*, *HLA-F*, *HLA-E*, *HLA-DRB6*, *HLA-DRB5*, *HLA-DRB1*, *HLA-DRA*, *HLA-DQB2*, *HLA-DQB1*, *HLA-DQA1*, *HLA-DPB2*, *HLA-DPB1*, *HLA-DPA1*, *HLA-DOB*, *HLA-DOA*, *HLA-DMB*, *HLA-DMA*, *HLA-C*, *HLA-B*, *HLA-A*), comprehensive analysis and comparisons were made, which exhibited their higher expressions in the immuno-active group (**Fig. 5B**).

In cervical cancers, mutation burden is associated with a good response to ICP therapy [20,21]. We analyzed the impact of mutation load and found that there were substantial differences between the 2 clusters we previously defined. IS Lo tended to have higher mutation load comparing with IS Hi (p=0.0096) (**Fig. 5C**), suggesting that patients with higher mutation load may gain better prognosis.

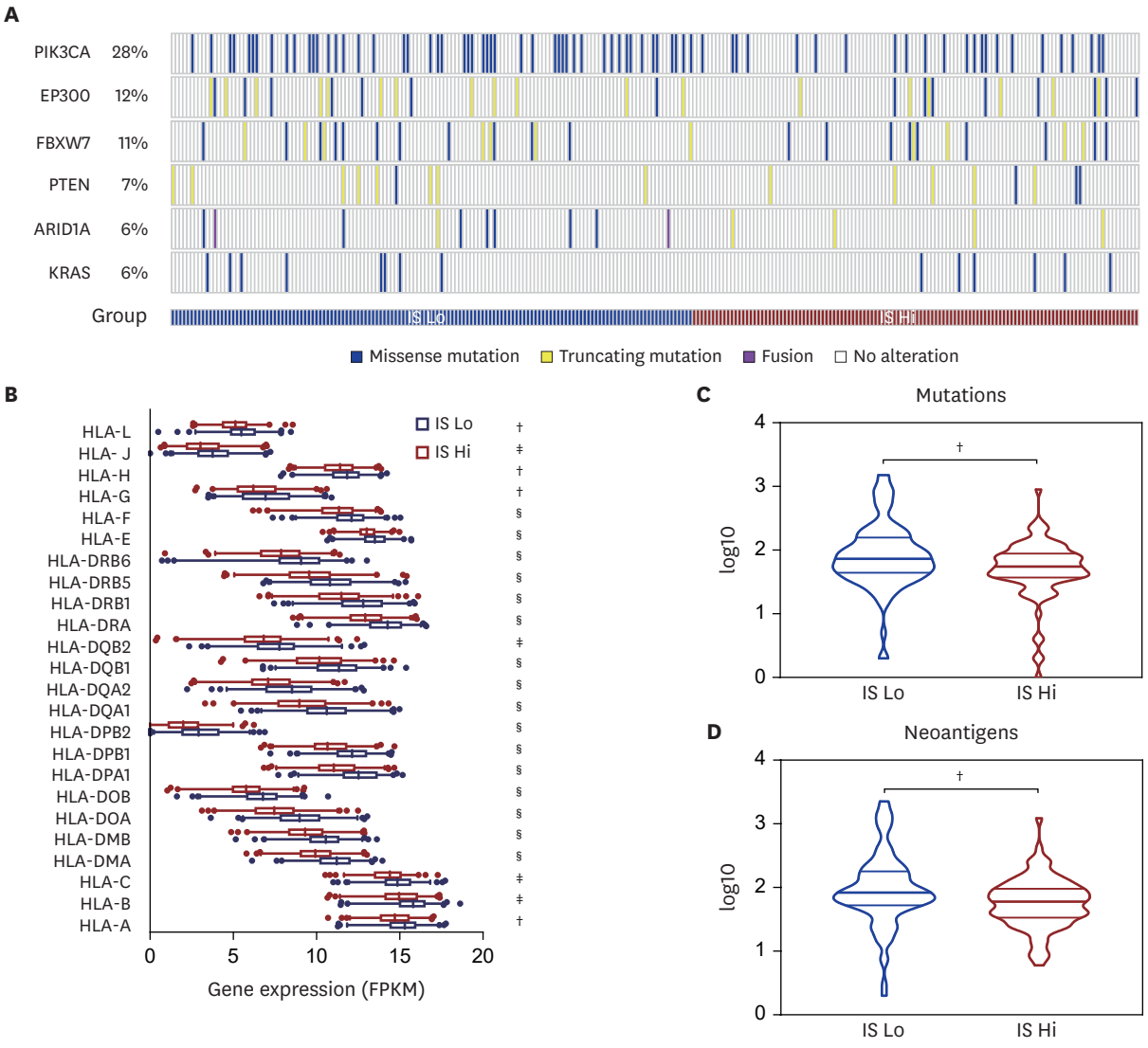

Fig. 5. Gene mutation landscape of cervical cancer. (A) Patients were categorized according to their common mutated genes. (B) Box plots of HLA expression between the 2 groups. Scatter plots showed IS Lo had higher (C) mutation load and (D) neoantigen load than IS Hi. (E) Somatic mutation differences between IS Lo and IS Hi. (F) Sector graph showed different proportions of *PIK3CA* mutational status in IS Lo and IS Hi. (G) Violin plots of IS in PIK3CA^{mutated} and PIK3CA$^{wild\ type}$. (H) Violin plots of ICPs expression based on PIK3CA mutational status.
CI, confidence interval; ICP, immune checkpoint; IS, immunoscore; OR, odds ratio.
*p<0.05; †p<0.01; ‡p<0.001; §p<0.0001.

(continued to the next page)

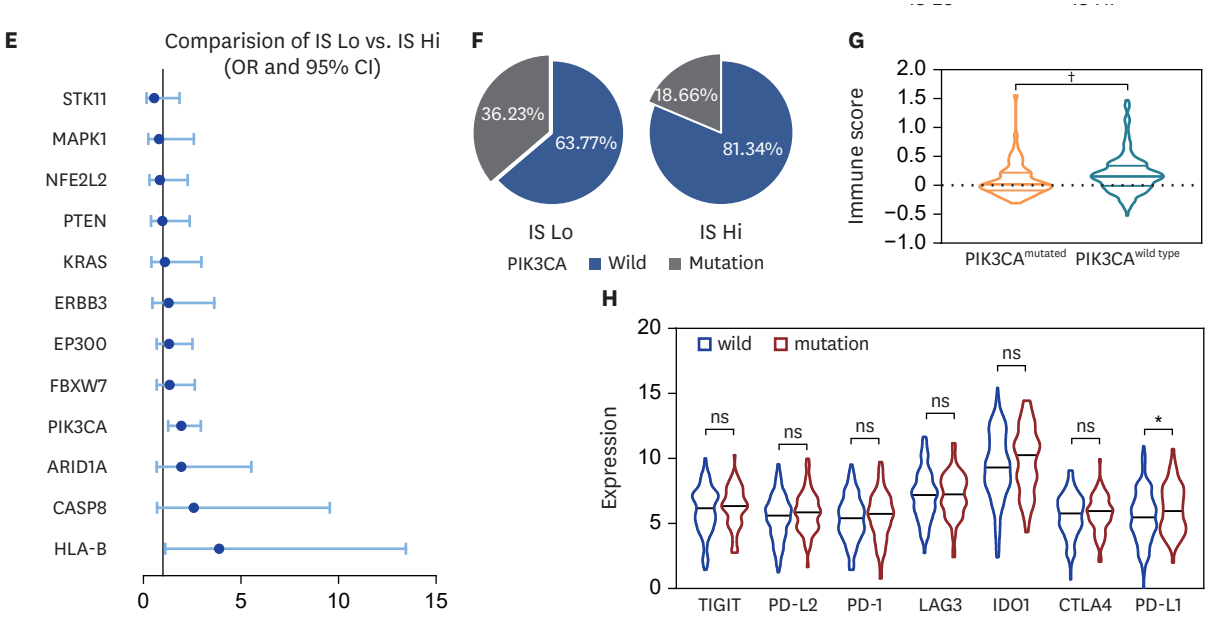

Fig. 5. (Continued) Gene mutation landscape of cervical cancer. (A) Patients were categorized according to their common mutated genes. (B) Box plots of HLA expression between the 2 groups. Scatter plots showed IS Lo had higher (C) mutation load and (D) neoantigen load than IS Hi. (E) Somatic mutation differences between IS Lo and IS Hi. (F) Sector graph showed different proportions of *PIK3CA* mutational status in IS Lo and IS Hi. (G) Violin plots of IS in PIK3CA^{mutated} and PIK3CA$^{wild\ type}$. (H) Violin plots of ICPs expression based on PIK3CA mutational status.
CI, confidence interval; ICP, immune checkpoint; IS, immunoscore; OR, odds ratio.
*p<0.05; †p<0.01; ‡p<0.001; §p<0.0001.

Since neoantigens are promising candidates for effective cancer vaccines [22], we analyzed neoantigen load in these 2 groups. Interestingly, we observed increasing neoantigens in IS Lo with better disease outcome (p=0.0019) (**Fig. 5D**), although the underlying mechanism is unclear. Nonetheless, these results suggested that the robust immune response in IS Lo was likely related to the effects of neoantigens.

4. PIK3CA might be a promising biomarker for the choice of treatment and prognosis

Upon checking the difference in frequency between IS Lo and IS Hi, we found that SMGs were not equally distributed in these 2 groups. Our study displayed that, *PIK3CA*, a frequent somatic mutation in cervical cancer, was more likely to be mutated in IS Lo in cervical cancer (a 2-tailed Fisher's exact p-value=0.002) (**Fig. 5E**). To be more specific, PIK3CA^{mutated} with lower IS (**Fig. 5G**) was detected in IS Lo of 50 (36.23%) patients and IS Hi of 25 (18.66%) patients (**Fig. 5F**).

Since immunological checkpoint inhibitors (involving anti-PD1 and anti-PDL1 agents) are being developed, we then looked at the distribution of ICPs expression between the 2 groups. Intriguingly, patients with *PIK3CA* mutations were discovered a higher expression of *PD-L1* (**Fig. 5H**). Conceivably, the connection between PIK3CA mutations and *PD-L1* expression suggested its potential possibility of drug utilization, such as PD-1 or PD-L1 inhibitors [14,20].

DISCUSSION

Given numerous studies have focused on the indicators or biomarkers for prognosis prediction, a more effective prognosis model is still desperately needed. In the meantime,

https://doi.org/10.3802/jgo.2021.32.e32

our studies identify an IS signature consisting of 5 immune cells with LASSO Cox regression analysis, which is significantly superior to apply FIGO staging alone. According to our classification based on IS, the ICPs inhibitors and PI3K inhibitors may become the potential treatments towards the low IS group. In conclusion, this preliminary study seems to facilitate patient risk stratification and optimize therapy in cervical cancers.

Based on previous research, those with high immune infiltrates tumors have better outcomes with conventional therapy or immunotherapy [23,24]. In this study, our first intriguing observation is that, of 23 cells including fibro, not all but 5 specific selected cells contribute to build the new prognostic model. In the ultimate formula based on LASSO Cox regression method, Neut, Masta, macrophages (M0) were considered as worse prognostic indicators while CD8T was considered as a favorable prognostic indicator. We also noticed that NK cell-mediated cytotoxicity and T-cell receptor signaling pathway were upregulated in IS Lo which was defined as an immuno-active cluster. These finding were consistent with previous studies [25-27]. Furthermore, we got an IS "immunoscore" on the basis of LASSO Cox Regression method. Multivariate Cox analysis and ROC curve, combining FIGO staging and IS, manifested the advantage of IS over cervical cancer to predict survival, indicating its promising prospect of clinical application. In addition, we analyzed the fraction of immune infiltrates in these 2 groups based on MCP-counter, which assists in accessing the immune composition of a tumor sample. In accordance with the results before, we found that CD8T, B cells and mono were abundant in cervical cancers. Interestingly, our results revealed that the higher infiltration of myeloid cells, which contributed to malignant transformation as well as cancer progression and metastasis [28], had been observed in IS Lo, indicating the variation and complexity of TME. In this case, IHC for 5 related cells was performed: Neut, Mast cells, Macrophages, NK cells, CD8T. Then, samples from patients was categorized into 2 groups by applying Hierarchical Clustering (**Supplementary Fig. 3A**). Notably, a higher expression level of GZMB was seen in the group with higher aggregation of CD8T (**Supplementary Fig. 3B**). Despite the inconsistent immune infiltrates, it revealed the promising clinical value of those 5 specific cells for prognostic prediction. However, how every cell out of the 5 exerts an impact on prognosis remained further experiments, owing to limits that the formula we constructed was based on the TCGA database and our sizes of the population were relatively limited. Therefore, further studies are needed to explore intrinsic features of TICs and their clinical significance in cervical cancer.

Besides, there were significant differences in mutation and neoantigen loads between the 2 groups. Neoantigens are extremely unique and their selective expression on tumor cells greatly lower the risk of autoimmunity and immune tolerance. Recently, several studies also revealed that highly mutated tumors are more likely to possess neoantigens, making them become targets, activate immune cells and respond to therapeutic strategies [29-31]. According to our study, IS Lo with higher level of mutation load and neoantigen loads showed a better OS while IS Hi was correlated with a worse clinical outcome, which might partly explain the good response to treatments in cervical cancer and indicated its clinical value. Meanwhile, our preliminary results showed that *HLA* family genes are usually much higher expressed in immuno-active samples of cervical cancer. Prior studies have shown that loss of *HLA* gene family especially *HLA-I* are involved in distinct biological processes including tumor progression and resistance to immunotherapy [32,33]. In addition, downregulation of *HLA* genes may facilitate immune evasion, for a pivotal step in neoantigen presentation and cytolytic T cell response is governed by *HLA*, especially class I *HLA.* In summary, we supposed that higher expression of *HLA* may relate to stronger immune activity, which made it possible to be a promising predictive biomarker of survival.

As the advances of immunotherapy, more related drugs have been developed. However, a certain number of patients failed to response in clinical practice [34-36]. Until now, several studies have demonstrated that PD-1 and PD-L1 expression were favorable prognostic indicators while others denied, and thus the results still remained controversial [39,40]. Our study showed a positive effect of PD-1 and PD-L1. Meanwhile, we found stronger expression of GZMB in patients who had higher expression of PD-1 and PD-L1, suggesting its stronger anti-tumor response. Similar results have also been observed in other gynecologic cancers like ovarian cancer [40]. We speculated that this phenomenon might be explained by compensatory upregulation to coordinate the TME, though the in-detail mechanisms were still not clearly understood. As PD-L1 expression pattern is more complicated, we evaluated every point of TMA separately according to different sites. Comparing with PD-L1+ tumor cells, PD-L1+ tumor infiltrating lymphocytes displayed stronger correlation with the expression of GZMB, which might be a better indicator to predict prognosis, implying the activation of anti-tumor response in tissues. Meanwhile, we also noticed increase in PD-1, PD-L1 and GZMB expression were significantly correlated with the progression of disease, from CIN to cervical cancer (**Supplementary Fig. 2E and F**), which corresponded with previous research [41,42]. However, there was no significant difference in HPV status between the 2 groups after analyzing our own data (**Supplementary Fig. 2G**).

Additionally, *PIK3CA*, one of the most frequently mutated genes, is known to play a vital role in regulating cell growth and apoptosis. Higher expression of *PD-L1* in PIK3CA^{mutated} patients showed the potential and possibility to response to PD-1 or PD-L1 inhibitors in cervical cancers before [43,44], and we might need additional research to support the assumption. Some limitations should be addressed. It was a retrospective study and the sizes of the population were relatively limited. Additional studies are required.

In conclusion, our investigations constructed a new prognostic model by selecting several immune infiltrating cells and identified a new IS, which might be an effective predictive tool to distinguish patients who might benefit from therapeutic strategies. The low IS group along with higher expression of ICPs might be a crucial indicator for immunotherapy and better prognosis. Also, there is also an opportunity to develop PI3K inhibitors and provide insights into immunotherapy resistance.

SUPPLEMENTARY MATERIALS

Supplementary Table 1

Clinical characteristics and pathological information for patients in 3 clusters

Click here to view

Supplementary Table 2

Clinical characteristics and pathological information for patients in the 2 groups

Click here to view

Supplementary Table 3

Complementary information on pathway enrichment analysis

Click here to view

https://doi.org/10.3802/jgo.2021.32.e32

JOURNAL OF GYNECOLOGIC ONCOLOGY

Supplementary Fig. 1

Clinical information of 3 clusters. The histogram of (A) Pathological type, (B) HPV status, (C) HPV types in cluster 1, 2, and 3. Kaplan-Meier survival curves displayed the clinical outcomes stratified by FIGO staging in (D) Cohort 1, (E) IS Lo, (F) IS Hi.

Click here to view

Supplementary Fig. 2

Association between the expression of PD-L1 and GZMB. Correlation of PD-L1 and GZMB expression in Cohort 1 (A), Cohort 2 at specific areas: (B) total, (C) tumor core, (D) stroma. Different expression of PD-1, PD-L1, GZMB between patients of CINs and cancers in Cohort 2 (E), Cohort3 (F), between HPV+ and HPV− in Cohort 2 (G).

Click here to view

Supplementary Fig. 3

Clinical application of IS. Images of IHC for (A) CD8T, (B) CD68, (C) anti-mast cell tryptase, (D) CD66b, (E) CD56 in TMA. (F) Cohort 2 was categorized into 2 groups by applying Hierarchical Clustering. (G) Violin plots of GZMB expression per HPF between the 2 groups.

Click here to view

REFERENCES

1. Bray F, Ferlay J, Soerjomataram I, Siegel RL, Torre LA, Jemal A. Global cancer statistics 2018: GLOBOCAN estimates of incidence and mortality worldwide for 36 cancers in 185 countries. CA Cancer J Clin 2018;68:394-424.
PUBMED | CROSSREF
2. Hall MT, Simms KT, Lew JB, Smith MA, Saville M, Canfell K. Projected future impact of HPV vaccination and primary HPV screening on cervical cancer rates from 2017-2035: example from Australia. PLoS One 2018;13:e0185332.
PUBMED | CROSSREF
3. Minion LE, Tewari KS. Cervical cancer - State of the science: from angiogenesis blockade to checkpoint inhibition. Gynecol Oncol 2018;148:609-21.
PUBMED | CROSSREF
4. Li C, Ma C, Zhang W, Wang J. The immune function differences and high-risk human papillomavirus infection in the progress of cervical cancer. Eur J Gynaecol Oncol 2014;35:557-61.
PUBMED
5. Walch-Rückheim B, Ströder R, Theobald L, Pahne-Zeppenfeld J, Hegde S, Kim YJ, et al. Cervical cancer-instructed stromal fibroblasts enhance IL23 expression in dendritic cells to support expansion of Th17 cells. Cancer Res 2019;79:1573-86.
PUBMED | CROSSREF
6. Schreiber RD, Old LJ, Smyth MJ. Cancer immunoediting: integrating immunity's roles in cancer suppression and promotion. Science 2011;331:1565-70.
PUBMED | CROSSREF
7. Huang QT, Man QQ, Hu J, Yang YL, Zhang YM, Wang W, et al. Prognostic significance of neutrophil-to-lymphocyte ratio in cervical cancer: a systematic review and meta-analysis of observational studies. Oncotarget 2017;8:16755-64.
PUBMED | CROSSREF
8. Yang S, Wu Y, Deng Y, Zhou L, Yang P, Zheng Y, et al. Identification of a prognostic immune signature for cervical cancer to predict survival and response to immune checkpoint inhibitors. OncoImmunology 2019;8:e1659094.
PUBMED | CROSSREF

9. Chen Z, Han Y, Song C, Wei H, Chen Y, Huang K, et al. Systematic review and meta-analysis of the prognostic significance of microRNAs in cervical cancer. Oncotarget 2018;9:17141-8.
PUBMED | CROSSREF
10. Zeng D, Li M, Zhou R, Zhang J, Sun H, Shi M, et al. Tumor microenvironment characterization in gastric cancer identifies prognostic and immunotherapeutically relevant gene signatures. Cancer Immunol Res 2019;7:737-50.
PUBMED | CROSSREF
11. Fu H, Zhu Y, Wang Y, Liu Z, Zhang J, Xie H, et al. Identification and validation of stromal immunotype predict survival and benefit from adjuvant chemotherapy in patients with muscle-invasive bladder cancer. Clin Cancer Res 2018;24:3069-78.
PUBMED | CROSSREF
12. Arafeh R, Samuels Y. PIK3CA in cancer: the past 30 years. Semin Cancer Biol 2019;59:36-49.
PUBMED | CROSSREF
13. Lou H, Villagran G, Boland JF, Im KM, Polo S, Zhou W, et al. Genome analysis of Latin American cervical cancer: frequent activation of the PIK3CA pathway. Clin Cancer Res 2015;21:5360-70.
PUBMED | CROSSREF
14. Verret B, Cortes J, Bachelot T, Andre F, Arnedos M. Efficacy of PI3K inhibitors in advanced breast cancer. Ann Oncol 2019;30:X12-20.
CROSSREF
15. Bhatla N, Berek JS, Cuello Fredes M, Denny LA, Grenman S, Karunaratne K, et al. Revised FIGO staging for carcinoma of the cervix uteri. Int J Gynaecol Obstet 2019;145:129-35.
PUBMED | CROSSREF
16. Tibshirani R. The lasso method for variable selection in the Cox model. Stat Med 1997;16:385-95.
PUBMED | CROSSREF
17. Becht E, Giraldo NA, Lacroix L, Buttard B, Elarouci N, Petitprez F, et al. Estimating the population abundance of tissue-infiltrating immune and stromal cell populations using gene expression. Genome Biol 2016;17:218.
PUBMED | CROSSREF
18. Gene Ontology Consortium. Gene Ontology Consortium: going forward. Nucleic Acids Res 2015;43:D1049-56.
PUBMED | CROSSREF
19. Cancer Genome Atlas Research NetworkAlbert Einstein College of MedicineAnalytical Biological ServicesBarretos Cancer HospitalBaylor College of MedicineBeckman Research Institute of City of Hope Integrated genomic and molecular characterization of cervical cancer. Nature 2017;543:378-84.
PUBMED | CROSSREF
20. Ojesina AI, Lichtenstein L, Freeman SS, Pedamallu CS, Imaz-Rosshandler I, Pugh TJ, et al. Landscape of genomic alterations in cervical carcinomas. Nature 2014;506:371-5.
PUBMED | CROSSREF
21. Chen YP, Zhang Y, Lv JW, Li YQ, Wang YQ, He QM, et al. Genomic analysis of tumor microenvironment immune types across 14 solid cancer types: immunotherapeutic implications. Theranostics 2017;7:3585-94.
PUBMED | CROSSREF
22. Schumacher TN, Schreiber RD. Neoantigens in cancer immunotherapy. Science 2015;348:69-74.
PUBMED | CROSSREF
23. Naito Y, Saito K, Shiiba K, Ohuchi A, Saigenji K, Nagura H, et al. CD8+ T cells infiltrated within cancer cell nests as a prognostic factor in human colorectal cancer. Cancer Res 1998;58:3491-4.
PUBMED
24. Tumeh PC, Harview CL, Yearley JH, Shintaku IP, Taylor EJ, Robert L, et al. PD-1 blockade induces responses by inhibiting adaptive immune resistance. Nature 2014;515:568-71.
PUBMED | CROSSREF
25. Matsumoto Y, Mabuchi S, Kozasa K, Kuroda H, Sasano T, Yokoi E, et al. The significance of tumor-associated neutrophil density in uterine cervical cancer treated with definitive radiotherapy. Gynecol Oncol 2017;145:469-75.
PUBMED | CROSSREF
26. Krishnan V, Schaar B, Tallapragada S, Dorigo O. Tumor associated macrophages in gynecologic cancers. Gynecol Oncol 2018;149:205-13.
PUBMED | CROSSREF
27. Liang Y, Lü W, Zhang X, Lü B. Tumor-infiltrating CD8+ and FOXP3+ lymphocytes before and after neoadjuvant chemotherapy in cervical cancer. Diagn Pathol 2018;13:93.
PUBMED | CROSSREF
28. Schröer N, Pahne J, Walch B, Wickenhauser C, Smola S. Molecular pathobiology of human cervical high-grade lesions: paracrine STAT3 activation in tumor-instructed myeloid cells drives local MMP-9 expression. Cancer Res 2011;71:87-97.
PUBMED | CROSSREF

29. Rizvi NA, Hellmann MD, Snyder A, Kvistborg P, Makarov V, Havel JJ, et al. Cancer immunology. Mutational landscape determines sensitivity to PD-1 blockade in non-small cell lung cancer. Science 2015;348:124-8.
PUBMED | CROSSREF
30. Diaz LA Jr, Le DT. PD-1 blockade in tumors with mismatch-repair deficiency. N Engl J Med 2015;373:1979.
PUBMED | CROSSREF
31. Yarchoan M, Johnson BA 3rd, Lutz ER, Laheru DA, Jaffee EM. Targeting neoantigens to augment antitumour immunity. Nat Rev Cancer 2017;17:209-22.
PUBMED | CROSSREF
32. Flores-Martín JF, Perea F, Exposito-Ruiz M, Carretero FJ, Rodriguez T, Villamediana M, et al. A combination of positive tumor HLA-I and negative PD-L1 expression provides an immune rejection mechanism in bladder cancer. Ann Surg Oncol 2019;26:2631-9.
PUBMED | CROSSREF
33. Garrido F. HLA class-I expression and cancer immunotherapy. Adv Exp Med Biol 2019;1151:79-90.
PUBMED | CROSSREF
34. Chung HC, Ros W, Delord JP, Perets R, Italiano A, Shapira-Frommer R, et al. Efficacy and safety of pembrolizumab in previously treated advanced cervical cancer: results from the phase II KEYNOTE-158 study. J Clin Oncol 2019;37:1470-8.
PUBMED | CROSSREF
35. Liu JF, Gray KP, Wright AA, Campos S, Konstantinopoulos PA, Peralta A, et al. Results from a single arm, single stage phase II trial of trametinib and GSK2141795 in persistent or recurrent cervical cancer. Gynecol Oncol 2019;154:95-101.
PUBMED | CROSSREF
36. Frenel JS, Le Tourneau C, O'Neil B, Ott PA, Piha-Paul SA, Gomez-Roca C, et al. Safety and efficacy of pembrolizumab in advanced, programmed death ligand 1-positive cervical cancer: results from the phase Ib KEYNOTE-028 trial. J Clin Oncol 2017;35:4035-41.
PUBMED | CROSSREF
37. Bellmunt J, Mullane SA, Werner L, Fay AP, Callea M, Leow JJ, et al. Association of PD-L1 expression on tumor-infiltrating mononuclear cells and overall survival in patients with urothelial carcinoma. Ann Oncol 2015;26:812-7.
PUBMED | CROSSREF
38. Muenst S, Soysal SD, Gao F, Obermann EC, Oertli D, Gillanders WE. The presence of programmed death 1 (PD-1)-positive tumor-infiltrating lymphocytes is associated with poor prognosis in human breast cancer. Breast Cancer Res Treat 2013;139:667-76.
PUBMED | CROSSREF
39. Li Y, Liang L, Dai W, Cai G, Xu Y, Li X, et al. Prognostic impact of programed cell death-1 (PD-1) and PD-ligand 1 (PD-L1) expression in cancer cells and tumor infiltrating lymphocytes in colorectal cancer. Mol Cancer 2016;15:55.
PUBMED | CROSSREF
40. Darb-Esfahani S, Kunze CA, Kulbe H, Sehouli J, Wienert S, Lindner J, et al. Prognostic impact of programmed cell death-1 (PD-1) and PD-ligand 1 (PD-L1) expression in cancer cells and tumor-infiltrating lymphocytes in ovarian high grade serous carcinoma. Oncotarget 2016;7:1486-99.
PUBMED | CROSSREF
41. Yang W, Lu YP, Yang YZ, Kang JR, Jin YD, Wang HW. Expressions of programmed death (PD)-1 and PD-1 ligand (PD-L1) in cervical intraepithelial neoplasia and cervical squamous cell carcinomas are of prognostic value and associated with human papillomavirus status. J Obstet Gynaecol Res 2017;43:1602-12.
PUBMED | CROSSREF
42. Yang W, Song Y, Lu YL, Sun JZ, Wang HW. Increased expression of programmed death (PD)-1 and its ligand PD-L1 correlates with impaired cell-mediated immunity in high-risk human papillomavirus-related cervical intraepithelial neoplasia. Immunology 2013;139:513-22.
PUBMED | CROSSREF
43. Wang L, Liu Y, Zhou Y, Wang J, Tu L, Sun Z, et al. Zoledronic acid inhibits the growth of cancer stem cell derived from cervical cancer cell by attenuating their stemness phenotype and inducing apoptosis and cell cycle arrest through the Erk1/2 and Akt pathways. J Exp Clin Cancer Res 2019;38:93.
PUBMED | CROSSREF
44. Du G, Cao D, Meng L. miR-21 inhibitor suppresses cell proliferation and colony formation through regulating the PTEN/AKT pathway and improves paclitaxel sensitivity in cervical cancer cells. Mol Med Rep 2017;15:2713-9.
PUBMED | CROSSREF